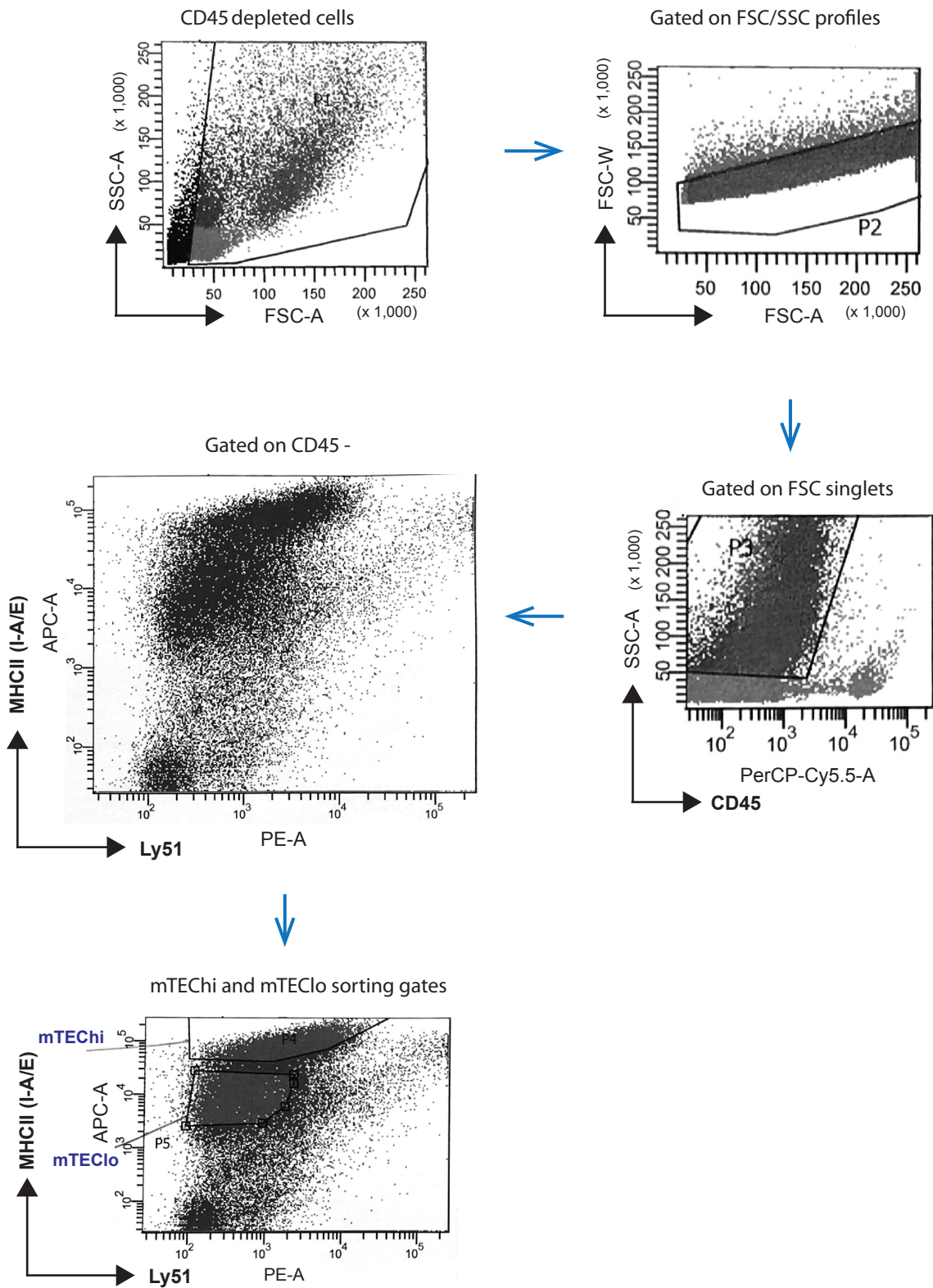


Appendix for “Aire-dependent transcripts escape Raver2-induced splice-event inclusion in the thymic epithelium”

Table of contents of Appendix figures

Appendix Figure S1	page 2
Appendix Figure S2	page 3
Appendix Figure S3	page 4
Appendix Figure S4	page 5
Appendix Figure S5	page 6
Appendix Figure S6	page 7
Appendix Figure S7	page 8
Appendix Figure S8	page 9
Appendix Figure S9	page 10

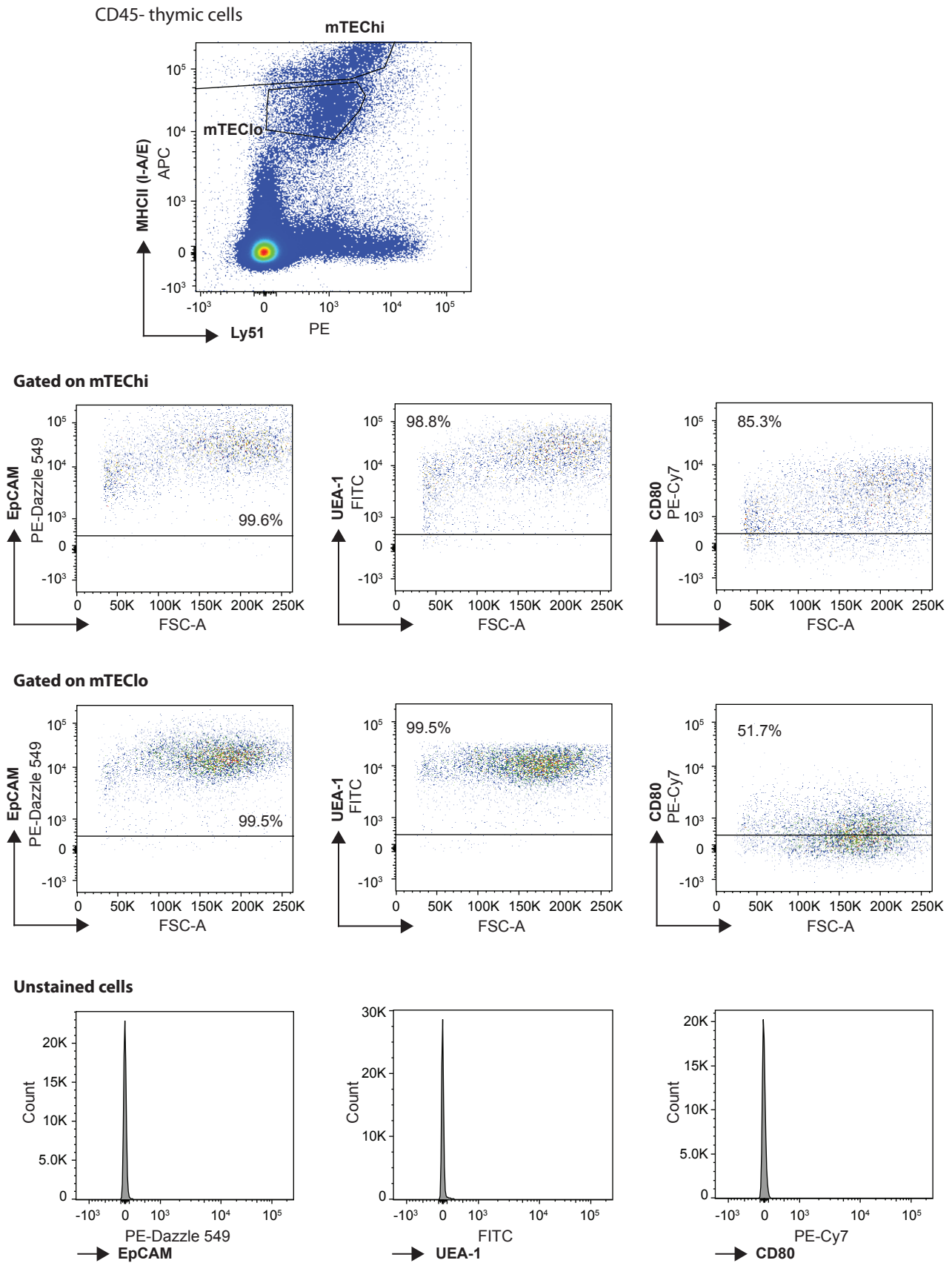
Figure S1



Appendix Figure S1. Gating strategy used to isolate mTEChi and mTEClo.

CD45 negative cells were separated based on the expression of Ly51 and MHCII (I-A/E). Low levels of Ly51 and high levels of MHCII mark mTEChi, whereas low levels of Ly51 and intermediate levels of MHCII mark mTEClo.

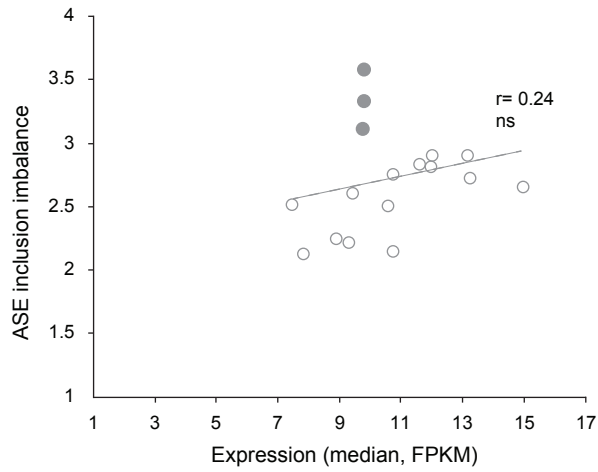
Figure S2



Appendix Figure S2. Phenotypic validation of the isolated mTEChi and mTEClo.

Levels of EpCAM, UEA-1 and CD80 at the surface of the isolated mTEChi and mTEClo are shown. Levels corresponding to the unstained cells are also represented.

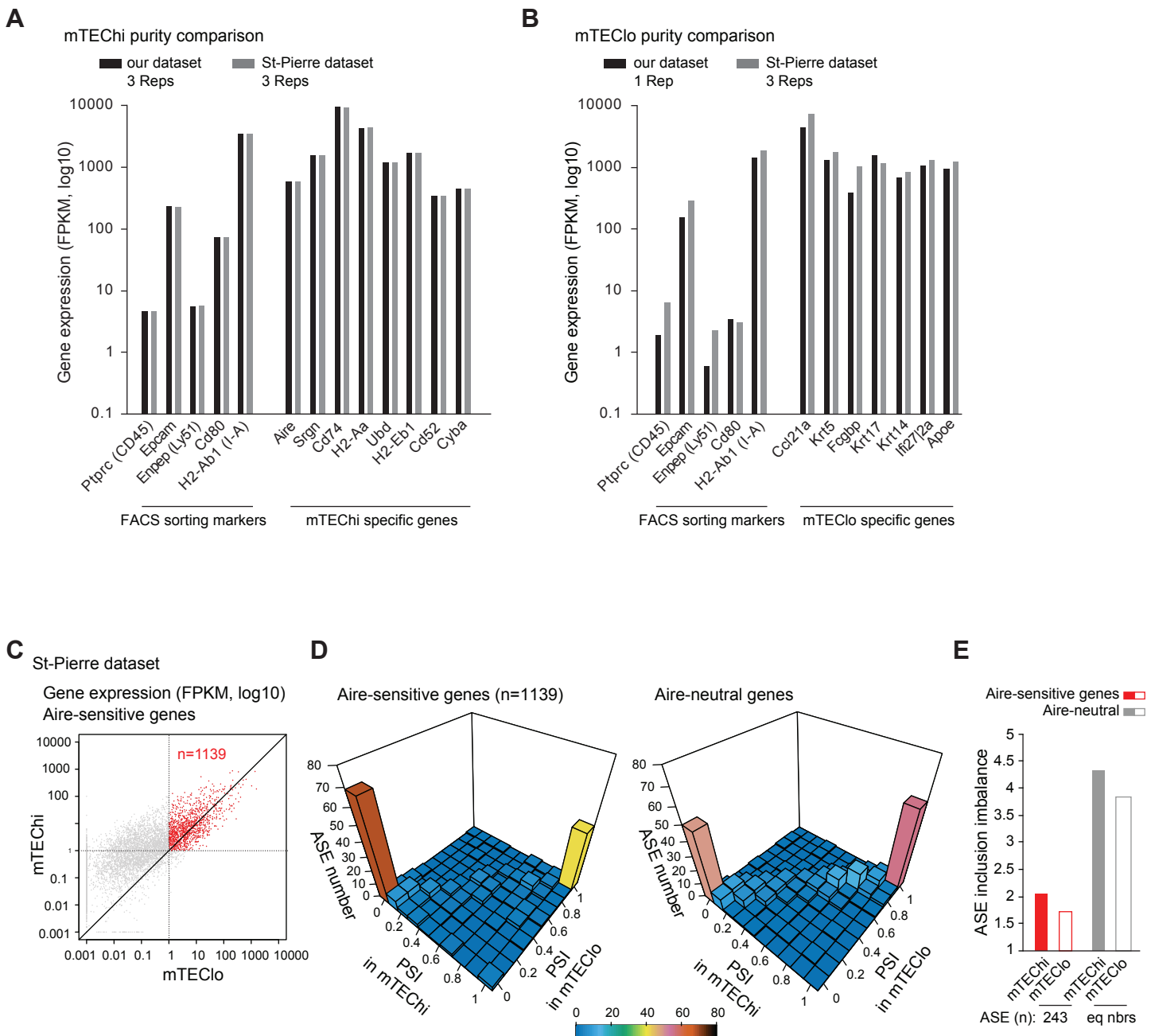
Figure S3



Appendix Figure S3. Lack of correlation between the levels of ASE inclusion imbalance and of expression of Aire-neutral genes across tissue and mTEChi samples.

Levels of ASE inclusion imbalance for Aire-neutral genes relative to their median gene expression in peripheral tissues (opened circles) and three mTEChi replicates (closed circles). The dashed line stands for the linear regression (not significant) across all samples. Pearson correlation.

Figure S4



Appendix Figure S4. ASE inclusion replication analysis in an independent mTEChi/lo RNA-seq dataset.

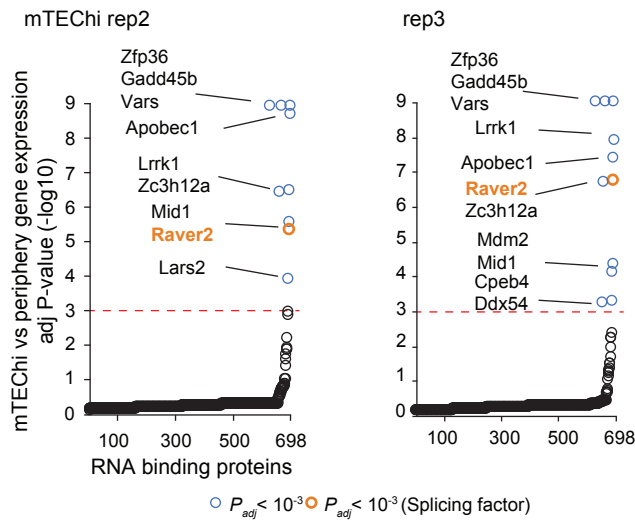
A, B Exact (**A**) and very close (**B**) levels of gene expression for the markers used to sort mTEChi and mTEClo in St-Pierre dataset and for mTEChi and mTEClo specific genes defined by re-analysis of the public scRNA-seq dataset generated in (Bornstein, Nature 2018); mean of n biological replicates (Reps).

C Differential gene expression of Aire-sensitive genes between mTEChi and mTEClo of St-Pierre dataset. Red dots show the Aire-sensitive genes with FPKM > 1 in mTEChi and mTEClo (n=1139). (3 mTEChi and 3 mTEClo replicates).

D 3D representation of the distribution of ASEs of Aire-sensitive (Left) and neutral genes (Right) according to their PSI values calculated from 3 mTEChi replicates (combined) and 3 mTEClo replicates (combined).

E Levels of ASE inclusion imbalance for Aire-sensitive and neutral genes (equal numbers) based on PSI values calculated from 3 mTEChi replicates (combined) and 3 mTEClo replicates (combined).

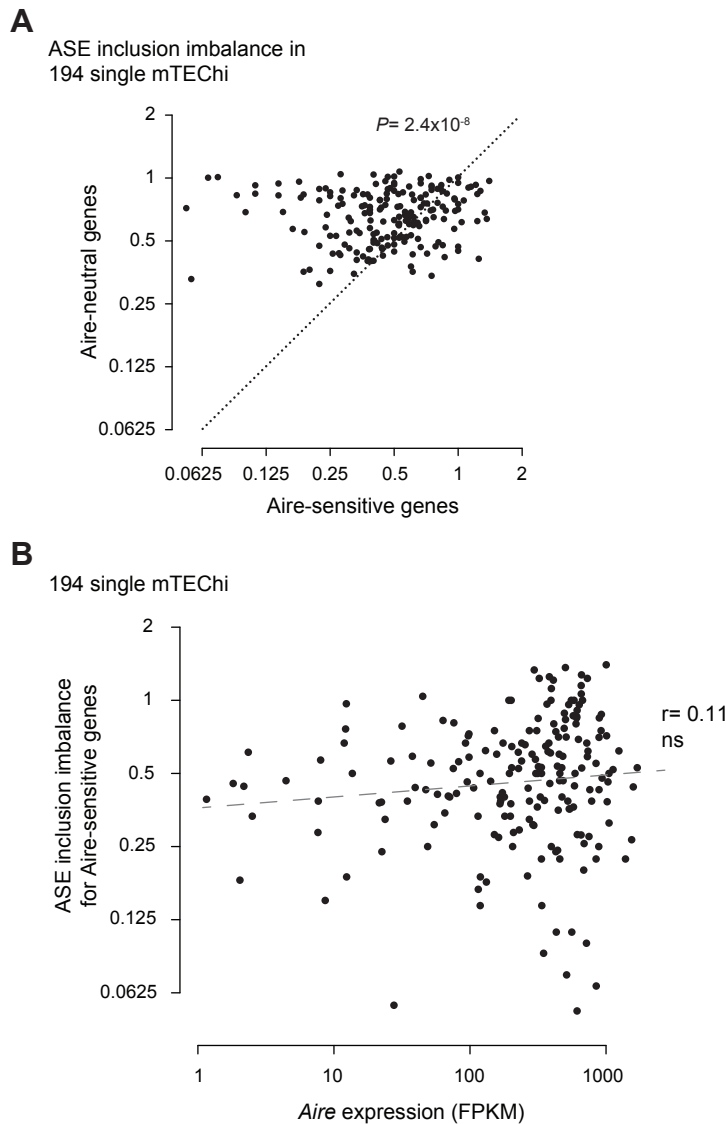
Figure S5



Appendix Figure S5. Differential expression of genes coding for RNA-binding proteins in two mTEChi replicates vs peripheral tissues.

The red dashed line represents the threshold for statistical significance (Benjamini-Hochberg adjusted $P < 0.001$). RNA-binding proteins showing significant differential gene expression are represented by colored circles, in orange if the RNA-binding proteins have been reported to be involved in splicing, in blue otherwise.

Figure S6

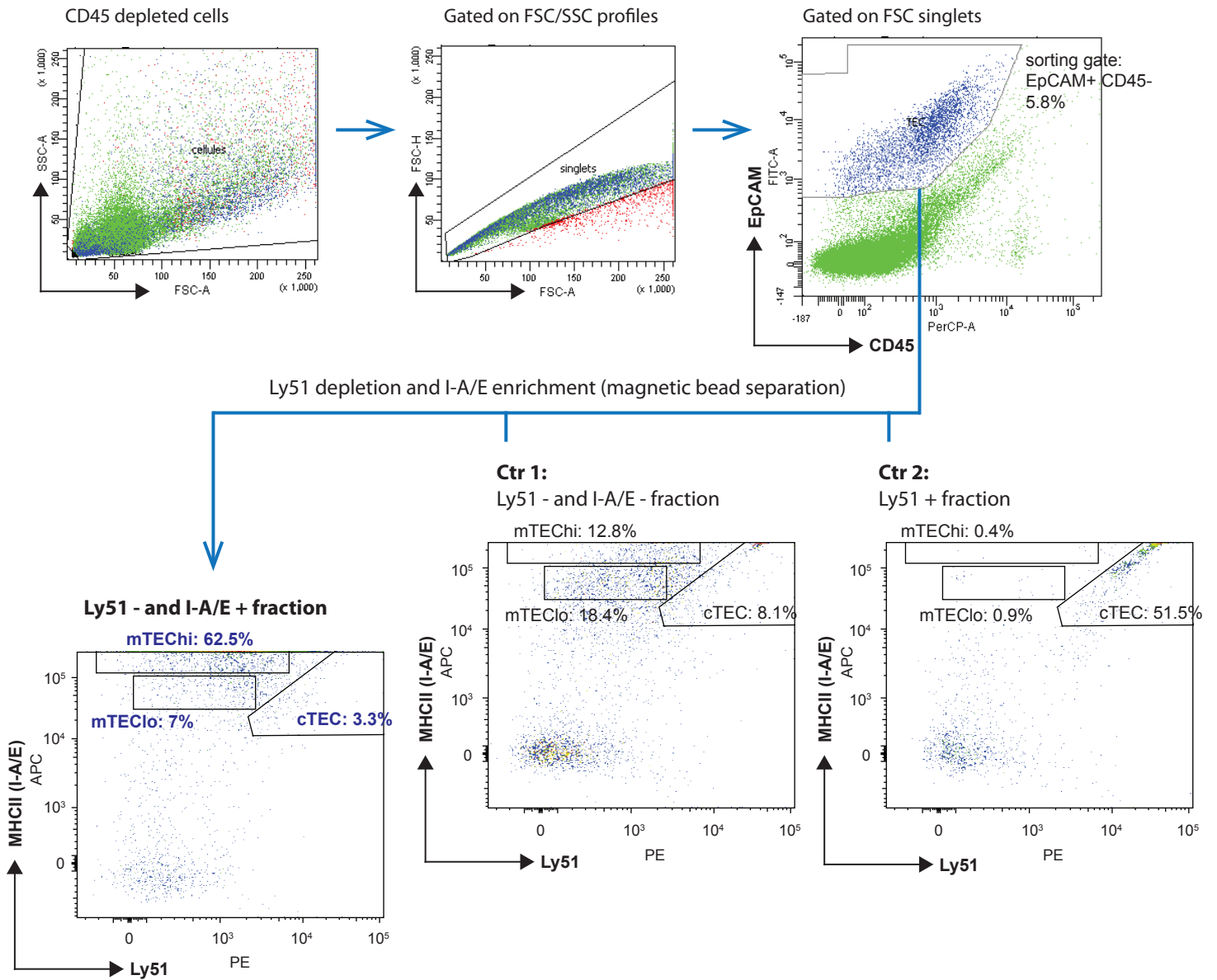


Appendix Figure S6. Low levels of ASE inclusion imbalance for Aire-sensitive genes in single mTEChi.

A Levels of ASE inclusion imbalance are shown for Aire-neutral and Aire-sensitive genes in 194 single mTEChi that are positive for Aire (FRKM > 1). The dotted diagonal line represents similar ASE inclusion for the two gene sets. The distribution of cells is significantly skewed towards lower levels of ASE inclusion imbalance for Aire-sensitive genes. Student's t-test.

B Levels of ASE inclusion imbalance for Aire-sensitive genes relative to their median gene expression in single mTEChi. The dashed line stands for the linear regression (not significant) across all samples. Pearson correlation.

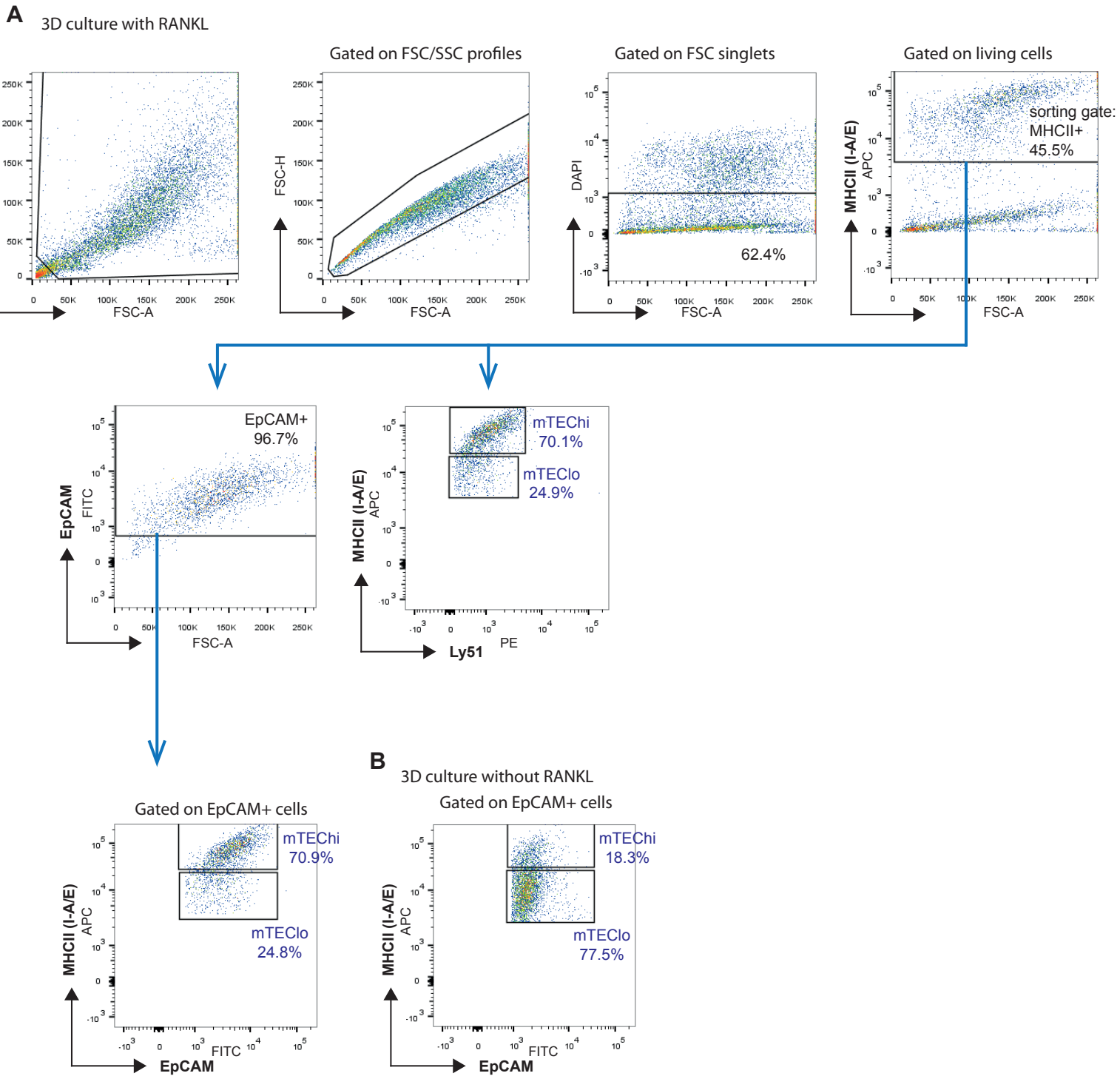
Figure S7



Appendix Figure S7. Gating strategy and TEC proportions seeded onto the 3D organotypic culture system.

The first row describes how the CD45 depleted thymic cells were selected and sorted depending on EpCAM expression and the absence of CD45 staining (EpCAM+ CD45- sorting gate). Following a depletion of Ly51 and an enrichment of I-A/E by magnetic bead separation, the obtained cells (in the Ly51- I-A/E+ fraction) show a proportion of mTEChi and mTEClo of about 62% and 7%, respectively, as well as a minority of cTECs (~3%). For comparison, TEC proportions in the other fractions are shown (Ctr1 and Ctr2).

Figure S8



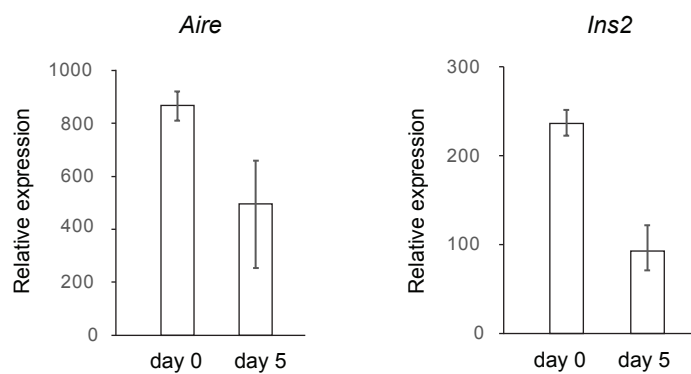
Appendix Figure S8. Gating strategy and TEC proportions retrieved from the 3D organotypic culture.

A The first row describes how the cells isolated from the 3D culture at day 5 were selected and sorted depending on I-A/E expression (MHCII⁺ sorting gate). These cells are almost entirely positive for EpCAM, and, based on MHCII and Ly51 expression, divide into about 70% mTEChi / 25% mTEClo.

B Proportions of mTEChi and mTEClo among MHCII⁺ EpCAM⁺ cells retrieved from 3D cultures performed without RANKL.

Figure S9

mTECs in the 3D system



Appendix Figure S9. Quantitation of Aire and Ins2 expression in mTECs before and after the 3D culture. qPCR measurement of Aire and Ins2 mRNA in mTECs seeded onto the 3D system (day 0) and after 5 days in culture (day 5). (n=3 biological replicates; error bars show mean \pm STD).